frontiers in Materials

ORIGINAL RESEARCH
published: 24 April 2019
doi: 10.3389/fmats.2019.00085

Cobalt Nanoparticles Encapsulated in Nitrogen-Doped Carbon Nanotube as Bifunctional-Catalyst for Rechargeable Zn-Air Batteries

Yang Liu[1,2], *Peng Dong*[2], *Mian Li*[2], *Hao Wu*[1,2], *Chengxu Zhang*[2], *Lina Han*[1,2]* *and Yingjie Zhang*[1,2]*

[1] School of Materials Science and Engineering, Kunming University of Science and Technology, Kunming, China, [2] National and Local Joint Engineering Laboratory for Lithium-ion Batteries and Materials Preparation Technology, Key Laboratory of Advanced Battery Materials of Yunnan Province, Kunming University of Science and Technology, Kunming, China

Developing economic and efficient non-noble-metal electrocatalysts toward oxygen reduction reaction (ORR) and oxygen evolution reaction (OER) is vitally important to improve the performance and economic outlook of alkaline-based rechargeable Zn-air battery technologies. In this work, a nitrogen-doped carbon nanotube encapsulated with metallic cobalt nanoparticles (Co@NC) was synthesized through a facile method and subsequent pyrolysis treatment. The field emission scanning electron microscope (FESEM), high resolution transmission electron microscopy (HRTEM), Raman spectra investigations demonstrate that the presence of Co induces the formation of carbon nanotube during the pyrolysis process and increase degree of graphitization of carbon nanotubes. The electrode activity is assessed by comparing OER with ORR indicators (ΔE). The ΔE value of Co@NC is 0.91 V, which is lower than the commercialized Pt/C (1.1 V) and nitrogen-doped carbon (NC) (1.17 V). The Co@NC-based primary Zn-air battery display an open circuit potential of 1.4 V, a high power density of 137 $mW{\cdot}cm^{-2}$, and outstanding energy density (708.3 $mAh{\cdot}kg_{Zn}^{-1}$ and 868.9 Wh kg_{Zn}^{-1} at 10 $mA{\cdot}cm^{-2}$), which batter than the commercialized Pt/C.

Keywords: bifunctional electrocatalyst, Co@NC, oxygen reduction reaction, oxygen evolution reaction, Zn-air battery

OPEN ACCESS

Edited by:
Jie-Sheng Chen,
Shanghai Jiao Tong University, China

Reviewed by:
Yaobing Wang,
Fujian Institute of Research on the Structure of Matter (CAS), China
Bao Yu Xia,
Huazhong University of Science and Technology, China
Zhang Jianan,
Zhengzhou University, China

***Correspondence:**
Lina Han
hanln2016@163.com
Yingjie Zhang
zyjkmust@126.com

Specialty section:
This article was submitted to Colloidal Materials and Interfaces, a section of the journal Frontiers in Materials

Received: *14 January 2019*
Accepted: *08 April 2019*
Published: *24 April 2019*

Citation:
Liu Y, Dong P, Li M, Wu H, Zhang C, Han L and Zhang Y (2019) Cobalt Nanoparticles Encapsulated in Nitrogen-Doped Carbon Nanotube as Bifunctional-Catalyst for Rechargeable Zn-Air Batteries. Front. Mater. 6:85. doi: 10.3389/fmats.2019.00085

INTRODUCTION

In response to the growing global energy demand and environmental crisis, extensive research has focused on energy conversion and storage devices. It is well-known that oxygen reduction reaction (ORR) and oxygen evolution reaction (OER) play a vital role in various energy storage systems, for instance, metal-air batteries (Park et al., 2016; Feng et al., 2018; Guo et al., 2018a; Wen et al., 2018) and fuel cells (He et al., 2013; Karim et al., 2017).

For this reason, excellent electrochemical performance Zn-air batteries need a bifunctional catalyst, which reveal excellent catalytic performance and stability, for ORR and OER. Traditionally, Platinum is deemed the best catalyst for ORR, while iridium is reputed the greatest catalyst for OER. However, some shortcomings such as exorbitant price, scarcity and poor stability have prohibited their extensive application (Deng et al., 2013; Dong et al., 2016; Tian et al., 2016; Qiao et al., 2017; Si et al., 2017).

To address above issue, various non-precious metal electrocatalyst, including transition metal oxides, transition metal nitrides, various carbon, and metal-free heteroatoms doped carbon were explored (Deng et al., 2015; Tao et al., 2015; Zhou et al., 2015; Cao et al., 2016; Qu et al., 2016, 2017; Yang Z. K. et al., 2016; Guo J. et al., 2017; Mo et al., 2017; Guo et al., 2018b; Liu et al., 2018). Among the various electrocatalysts being developed, CNT can not only improve electron transport, but also maintain and improve the stability of the catalyst under harsh conditions, which due to the metal cobalt encased in carbon nanotubes (Fang et al., 2016a; Guo S. et al., 2017; Sheng et al., 2017). Liu et al. adopted a hybrid strategy to synthesize carbon nanotubes and graphene as the carrier of metallic cobalt, and the catalyst also maintain high catalytic activity and stability under severe acidic conditions. Zheng et al. found that cobalt nanoparticles were wrapped in carbon nanotubes, which could prevent Co nanoparticles from being etched and oxidized in the post-process after pyrolysis, which have a pivotal part in enhancing the electrocatalyst stability to ORR and OER. Deng et al put forward a new idea to synthesize carbon nanotube encapsulated iron as ORR catalyst. In their opinion, the encapsulated metallic Fe can reduce the local work function of the surface carbon, which improve the ORR performance (Deng et al., 2017; Zhe et al., 2017; Zheng et al., 2017; Liu et al., 2018).

Recently, nitrogen-doped carbon nanotube has the potential to replace the metal-free-based electrocatalysts, which is mainly due to the nitrogen induced charge delocalization (Hao et al., 2017). Deng et al. obtained a suite of NCNTs by controlling the pyrolysis temperature of precursor polyaniline (PANI), which achieved the doping of nitrogen atoms into the carbon skeleton at the atomic level. By researching the unique electron configurations of carbon atoms in combination with different nitrogen functional groups, they found that nitrogen doping can provide atomic-level catalytic activity centers for ORR (Deng et al., 2017). Wang et al. developed an economical approach to obtain metallic Co encapsulated in N,S co-doped carbon nanotubes. the porous channels of the carbon skeleton provide more space for the dispersion of cobalt nanoparticles, and the introduction of nitrogen and sulfur into carbon nanotubes can provide more catalytic active sites (Wang et al., 2018). Zehtab et al. synthesized phosphorus functionalized carbon nanotubes (PCNTs) by heat treating CNT-H_3PO_4 at 170°C. The high phosphorus content and high specific surface area of PCNTs provided the corresponding conditions for improving the catalytic activity of ORR (Zehtab et al., 2015).

Recently, effective synthesis strategies are developed to accelerate the intensive research work of transition metal/nitrogen doped carbon nanotubes composites for ORR and OER. Song et al. obtained nitrogen-doped carbon nanotubes encapsulated cobalt nanoparticles catalyst by pyrolysis process, which showing preferable electrocatalytic performance. Li et al. conceived a method to synthesize *in situ*-generated Co@NCNTs derived from MOFs under H_2/Ar atmosphere. Jie et al. published a one-pot pyrolysis method to obtained N-doped carbon nanotubes encapsulated the synthesized nickel-cobalt alloy, which has high catalytic performance. Yang et al. designed a synthetic strategy using $FeCl_3/NH_3$ as the source to obtain Fe-N-C catalyst by heat-treating defective graphene at 950°C. Dilpazir et al. synthesized novel Co nanoparticles immobilized NCNTs on the zeolitic imidazolate framework treated with dicyandiamide (Yang X. et al., 2016; Jie et al., 2017; Li et al., 2017; Song et al., 2017; Dilpazir et al., 2018). However, in these experiments, the introduction of a template or the use of ammonia gas increased the cost and risk of the experiment.

Herein, cobalt acetate tetrahydrate ($Co(Ac)_2{\cdot}4H_2O$), dicyanamide (DCDA) and Poly(ethyleneglycol)-block-poly(propyleneglycol)-block-poly(ethyleneglycol) (P123) were elaborately selected to fabricate cobalt nanoparticles@N-doped carbon nanotubes composites (Co@NC). During the pyrolysis process, dicyanamide not merely do duty for a nitrogen source and carbon source and not only uses its reductivity to form the cobalt nanoparitcles. P123, serve as the main carbon source for the formation carbon nanotube structure under cobalt species inducing effect. In terms of its excellent overall catalytic performance for ORR and OER, the prepared Co@NC electrocatalyst is served as a cathode in rechargeable Zn-air battery and reveals a high specific power density, peak power density and stability, superior to that of the commercialized Pt/C.

EXPERIMENTAL SECTION

Chemicals

Cobalt acetate tetrahydrate ($Co(Ac)_2{\cdot}4H_2O$) was bought from Guangdong Guanghua Sci-Tech Co., Ltd. P123 (Mw = 5,800) and Nafion (5.0 wt %) were obtained from Sigma-Aldrich. Dicyandiamide (DCDA, 99.5%) was purchased from Acros. Concentrated hydrochloric acid (HCl, 37%) was bought from Chengdu Kelong Chemical Co., Ltb. Pt/C catalyst (20% Pt) was obtained from Shanghai Hesen Electric Co., Ltd. All the chemicals were used without further purification.

Synthesis of Co@NC Electrocatalysts

$Co(Ac)_2{\cdot}4H_2O$ and P123 were dissolved with H_2O and HCl in the 200 mL beaker. After stirring at 50°C for 12 h, the DCDA was added. The final molar ratio of $Co(Ac)_2{\cdot}4H_2O$: P123: DCDA: HCl: H_2O in the mixture was 0.003: 0.001: 1: 0.8: 13. Then the solution was dried at 50°C to obtain precursor. The bulk precursor was calcined in a tube furnace under the protection of a N_2 atmosphere. Firstly, it was arised to 400°C at a heating rate of 5°C/min and maintained 1 h, then the temperature further arised to 900°C at the same heating rate and maintained 1 h. In the preparation of the precursor, we performed an experiment without adding a cobalt source under the same synthesis conditions, and the obtained sample was named NC.

Electrochemical Measurements

Electrochemical measurements were performed on a Metrohm Autolab (Swiss Wantong Co. Ltd, Switzerland), using a typical three-electrode device. The rotation ring-disk electrode (RRDE, φ = 5 mm, Swiss Wantong Co., Ltd.) was used as working electrode, Ag/AgCl electrode was used as referode electrode and platinum foil was used as counter electrode. The fabrication of the working electrode was carried out as following: catalyst (5 mg)

was mixed with H_2O (0.8 mL), CH_3CH_2OH (0.2 mL) and Nafion solution (50 μL) in an ultrasonic bath to get evenly dispersed ink.

Then, 10 μL of the ink was dripped onto the glass carbon surface and natural drying at room temperature. The mass loading of catalyst on the surface of glass carbon electrode was 0.24 mg·cm^{-2}. All potentials in this paper are based on reversible hydrogen electrode potentials (RHE): $E_{RHE} = E_{Ag/AgCl} + 0.1976 + 0.0592 \times pH$ (Yang X. et al., 2016).

Cyclic voltammetry (CV) were measured in N_2-saturated or O_2-saturated 0.1 M KOH solution with a sweep rate of 10 mV·s^{-1}. The RDE and RRDE tests were carried out in O_2-saturated 0.1 M KOH solution at 1600 rpm with a scan rate of 10 mV·s^{-1}. The electrochemical impedance spectroscopy (EIS) of catalysts were measured in O_2-saturated KOH with 5 mV amplitude from 100 kHz to 0.01 Hz. NC and Pt/C catalyst were also measured using the same methods for comparison. All of the above electrochemical tests were performed at room temperature.

RESULTS AND DISCUSSION

Material Characterization of the Co@NC

The overall synthetic process of Co@NC is shown in **Figure 1a**. In the first step, nanorod colloid formed by P123 self-assembly in 2 M HCl solution containing amount of Co^{2+}. Secondary, DCDA with rich -NH_2, -NH and -C≡N functional group was added to obtain the precursor. Finally, the bulk precursor was annealed under N_2 atmosphere to obtain Co@NC. During precursor pyrolysis, carbon nanotube formed in the presence of cobalt, and Co^{2+} was reduced to Co nanoparticles encapsulated in carbon nanotube.

Field emission scanning electron microscope (FESEM) and TEM were used to investigate the as-obtained samples microstructure (**Figures 1b–d** and **Figures S2**, **S3**). The low resolution FESEM and TEM image (**Figures S2a**, **S3a**) indicate Co nanoparticles was encapsulated in carbon nanotube successfully, and the particle size of Co nanoparticles is within the scope of 20–100 nm. The width and length of carbon nanotube is about 200 nm and 10 μm, respectively. the interplanar spacing was about 0.203 nm (**Figure 1d**), corresponding to the distance between the (111) planes of cobalt particles. Moreover, cobalt nanoparticles can be observed clearly encapsulated by several graphene layers. The TEM elemental mapping images show an atomically uniform distribution of the C, N and Co elements in prepared Co@NC sample (**Figure 1e**).

XRD patterns of NC and Co@NC were shown in **Figure 2A**, three diffraction peaks at 44.2°, 51.5°, and 75.6° were indexed to the (111), (200), and (220) crystal planes of face-centered (fcc) Co (PDF# 15-0806) (Chen et al., 2016), which suggested that Co^{2+} was induced to cobalt successfully. Beyond that, a broad peak around 26°, corresponding to graphitized carbon (002) diffraction (Hao et al., 2017; Liang et al., 2019). And compared with NC, the C(002) diffraction peak strengthened, indicating the increased graphitization of the carbon in the presence of cobalt nanoparticles (Ai et al., 2018).

Raman measurements were then used to investigate the carbon defects and the degree of graphitization. In **Figure 2B**, two distinct peaks at 1,360 and 1590 cm^{-1} are associated with D and G bands, respectively. The area ratio between D and G bands (S_D/S_G) were calculated as 3.047 and 1.489 for NC and Co@NC, respectively. The results indicate that the existence of cobalt could improve the degree of graphitization, which will have a positive effect on its conductivity and catalytic activity (Dai et al., 2016). Three characteristic peaks of Co were observed around 475.6, 516, and 676 cm^{-1} by Raman spectroscopy, which correspond to classical vibration modes E_g, F_{2g}, and A_{1g} of Co, respectively (Jie et al., 2017; Li et al., 2017).

X-ray photoelectron spectroscopy (XPS) was carried out to analyse the chemical valence state and surface element composition of Co@NC and NC in **Figures 2C,D** and **Figures S6**, **S7**. The survey spectra revealed that NC only contains three elements of C, N, O, and C, N, O, Co were coexistent in Co@NC (**Figure S6**). The specific contents of all elements are summarized in **Table S1**. The high resolution C1s spectrum were deconvoluted into three peaks (**Figure S7a**): C-C (284.6 eV), C-O (285.4 eV), and C=O (286.5 eV) (Dilpazir et al., 2018). The high resolution C1s spectrum (**Figure 2C**) exhibits four types of *N* species at 398.5, 400.1, 401, 403.6 eV, which correspond to pyridinic N, pyrrolic N, graphitic N, and oxidized N (Zhao and Chen, 2015; Fang et al., 2016a; Zhou T. et al., 2017). The content of pyridinic N was also higher than that of the other three nitrogen species in Co@NC, higher content of pyridine N is expected to exhibit superior ORR performance (Wei et al., 2017). As shown in **Figure 2D**, high resolution Co2p spectrum shows two types of Co species at 780.3 and 795.8 eV, corresponding to metallic Co2p3/2 and Co2p1/2 (Zhou L. et al., 2017). This further suggested that Co^{2+} was induced to cobalt successfully used DCDA as reducing agent. The presence of Co^{2+} and Co^{3+} may be due to the oxidation of the surface of the sample exposed to air during the preparation process (Chen et al., 2016). According to the XPS results (Zhou L. et al., 2017), the relative content of Co in the Co@NC sample was calculated to be about 0.91 at%.

Electrochemical Performance for ORR and OER

The ORR catalytic activity of Co@NC and NC were measured by cyclic voltammetry (CV) in N_2-saturated and O_2-saturated 0.1 M KOH solution with a sweep rate of 10 mV·s^{-1}, firstly. The diffusion current density of Co@NC, NC and Pt/C (**Figure S8**) both increases significantly in the case of the introduction of O_2, which indicate the intrinsic ORR catalytic activity of the Co@NC and NC.

To gain further insights into the electrocatalytic behavior of Co@NC and NC toward ORR and OER, LSV curves were acquired in a conentional three-electrode device in the O_2-saturated 0.1 M KOH solution. As observed, Co@NC electrocatalyst has a conspicuous electrocatalytic performance, the onset potential and half-wave potential ($E_{1/2}$) are 0.89 and 0.81 V, respectively, which both higher than NC and IrO_2/C (0.84 V, 0.7 V). Compared with the review results in the literature (**Table S3**), the ORR activity of Co@NC is one of non-precious metal electrocatalysts in alkaline media.

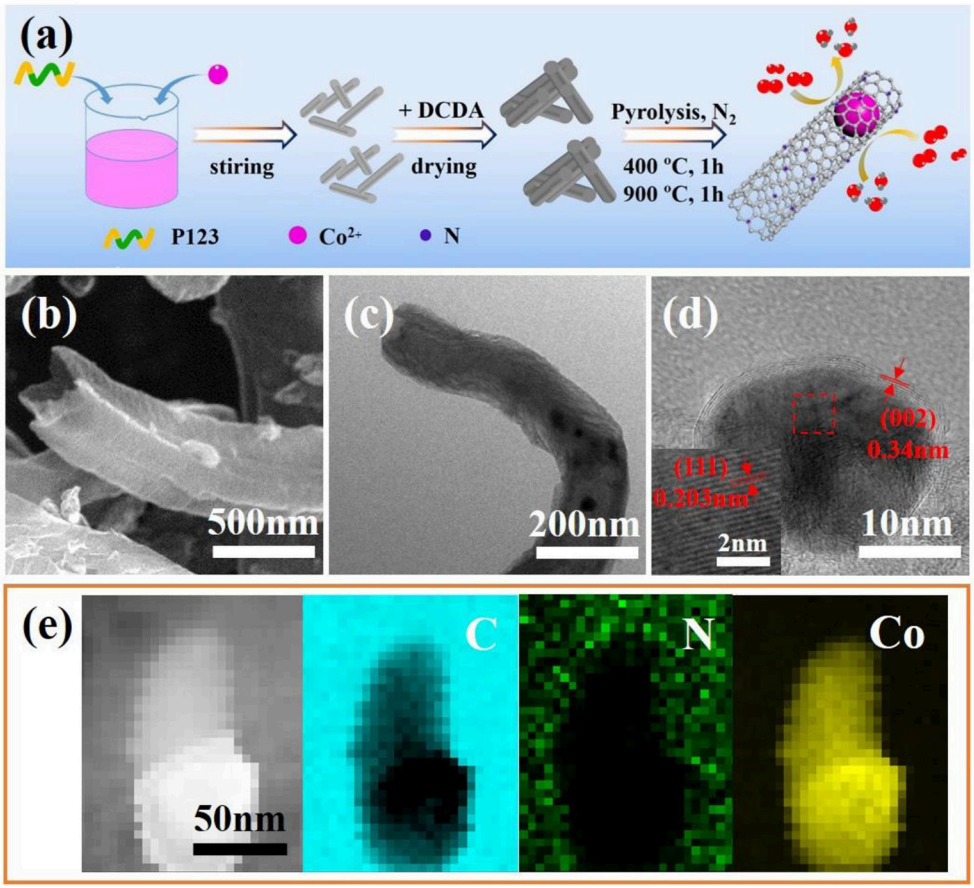

FIGURE 1 | (a) Schematic illustration of the overall synthetic process of Co@NC. **(b)** FESEM, **(c)** Transmission electron microscopy (TEM) and **(d)** HRTEM images of the Co@NC. **(e)** High angle annular dark field-scanning transmission electron microscope (HAADF-STEM) image and the corresponding elemental mapping of the Co@NC.

The Tafel slope was obtained from ORR polarization curves to evaluate the kinetic features of electrocatalysts, as shown in **Figure 3B**. The calculated Tafel slope of Co@NC (71 mV/dec) was close to Pt/C (61 mV/dec) and lower than NC (82 mV/dec) and IrO_2/C (103 mV/dec). The results suggested that the presence of cobalt can improve the degree of graphitization, thus increase the conductivity and decrease the slope of Tafel of Co@NC (Wang et al., 2016).

The catalytic activity of OER is customary assessed by comparing the potential at 10 mA·cm^{-2} (Qiao et al., 2016). As shown in **Figure 3A**, the Co@NC show the OER onset potential (1.47 V) and overpotential (0.5 V), which is comparable to the previously reported catalyst (**Table S3**). In addition, the Tafel slope was also calculated (**Figure 3C**), indicating the OER kinetics of the NC, Co@NC and Pt/C. The lower value of Tafel slope means a higher electrocatalysis performance for the OER. The Tafel slope of Co@NC is 110 mV/dec, lower than NC (163 mV/dec) and Pt/C (291 mV/dec), which suggest that the OER kinetics at Co@NC is faster than the other samples (Qiao et al., 2016). The turnover frequency (TOFs) was calculated to compare intrinsic activity (**Supporting Information**), the TOFs of the Co@NC and NC are 0.117 s^{-1} and 0.214 s^{-1} at an overpotential of 400 mV, respectively, and comparable to the previously reported noble-metal-free electrocatalyst in **Table S3**. Electrode activity can also be assessed by OER and ORR indicators differences ($\Delta E = E_{j=10} - E_{1/2}$), where the $E_{j=10}$ value is the corresponding OER potential at 10 mA·cm^{-2} (Meng et al., 2016). Co@NC shows the lowest ΔE value (0.91 V) compared with NC (1.1 V), Pt/C (1.17 V), and IrO_2/C (0.92 V), confirming the remarkable reversible oxygen electrode characteristics of Co@NC, which directly affects the charge-discharge performance of rechargeable Zn-air batteries (Kashyap and Kurungot, 2018).

To obtain more electrochemical kinetic information, the K-L plots of Co@NC, NC and Pt/C are obtained by K-L equation. **Figure 3D** shows the K-L plots calculated at 0.5 V at different speeds LSV curves. The K-L plots shows a good linearity between j^{-1} and $\omega^{-1/2}$, which indicated that the first-order reaction kinetics is closely related to the concentration of dissolved O_2 (Deng et al., 2017). The electron transfer numbers (n) of Co@NC, NC and Pt/C are calculated to be 3.74, 3.67, and 3.91, respectively, suggesting n is close to 4e$^-$ pathway for ORR (Zhang et al., 2015).

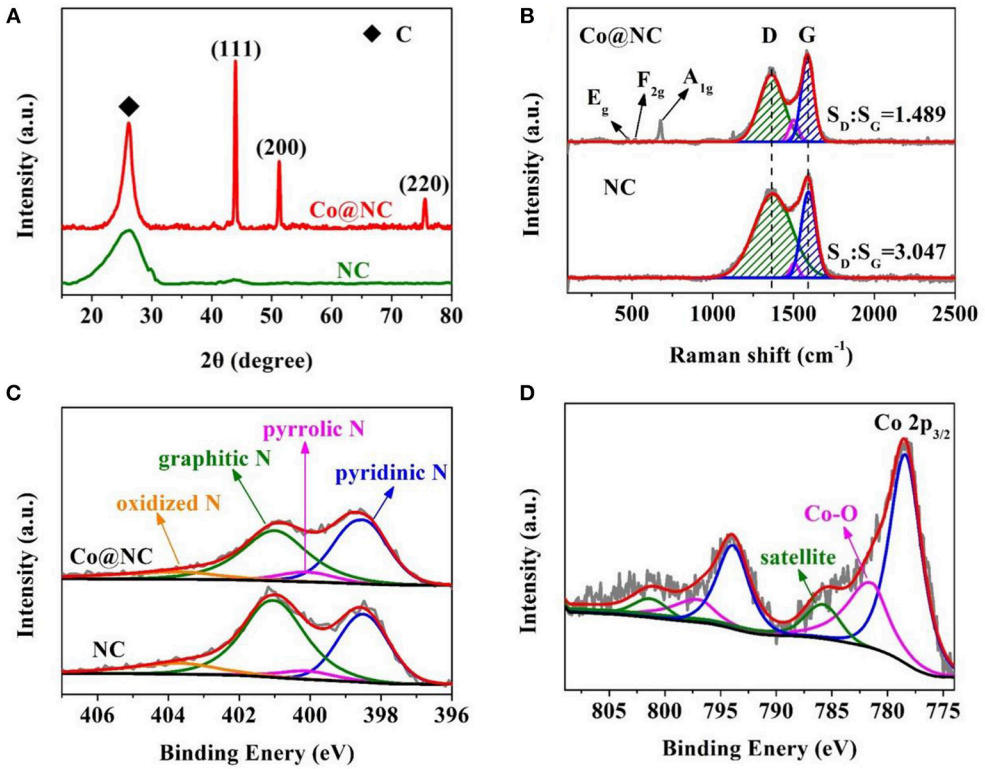

FIGURE 2 | (A) XRD patterns, **(B)** Raman spectra of NC and Co@NC. The high resolution spectrum of **(C)** N1s of NC and Co@NC. **(D)** The high resolution Co2p spectrum of Co@NC.

To further understand the reaction pathways and monitor the formation of peroxide, RRDE tests were carried out accurately calculate the amount of H_2O_2 generated. The proportion of H_2O_2 yield (**Figure S10**) and the electron transfer numbers (**Figure 4B**) of Co@NC, NC and commercial Pt/C were calculated according to disking current density and ring current density (**Figure 4A**). In the case of Co@NC electrocatalyst, the proportion of H_2O_2 yield is lower than 20%, and the n is higher than 3.5, which showed electrocatalytic selectivity was slightly lower than commercial Pt/C, consistenting with K-L plots results. Further suggest that Co@NC ideally performs oxygen reduction via $4e^-$ transfer pathway.

In addition, the stability of Co@NC electrocatalyst is a typical index to evaluate ORR performance, which is of great significance for the safe and stable operation of Zn-air batteries (Park et al., 2016). After accelerating aging process by continuously performing 200 cycles at 10 $mV{\cdot}s^{-1}$, the half-wave potential of Co@NC catalyst was merely 7 mV negative shift and its diffusion current density show no obvious decay (**Figure 4C**), which indicating significant electrochemical stability of Co@NC electrocatalyst. Comparatively speaking, the half-wave potential of NC catalyst has a negative shift of 10 mV and its diffusion current density decreased significantly.

To better understand the catalytic performance of Co@NC and the role played by N and Co, we further probed the active sites. Transition metals are very sensitive to SCN^- ions and can selectively attack the metal centers, impeding their catalytic activity. The ORR activity of Co@NC was re-examined in an electrolyte containing 5 mM KSCN. As shown in **Figure 4D**, we found that the onset potential, half wave potential and limited diffusion current density of Co@NC decreases in the presence of KSCN, suggesting a strong SCN^- ion coordination and blockage of the Co active sites (Amiinu et al., 2018). However, the onset potential, half wave potential and limited diffusion current density of NC was almost unchanged in the presence of SCN^- ions. We believe that both Co NPs and N-doped carbon play an important role in enhancing ORR catalytic performance. For the removal of Co NPs, the as-obtained material was also immersed in 0.5 M H_2SO_4 for 24 h. After washing with deionized water and ethanol for three times, the N-doped CNTs were obtained. As shown in supporting information **Figure S11**, we can know that Co@NC is more electrocatalytically active than N-doped CNTs. This comparison clearly shows that the N-C active site and Co NPs active site existed in Co@NC can significantly improve the catalytic activity (Guo et al., 2018a).

Electrochemical impedance spectroscopy (EIS) showed that the equivalent series resistance of Co@NC was smaller than NC (**Figure S12**), and there was no high frequency semicircle indicating that charge transfer resistance at the NC/electrolyte and Co@NC/electrolyte interface can be ignored, corresponding to a faster reaction rate. This indicates that the Co@NC has higher conductivity than NC, which corresponds to the Raman results.

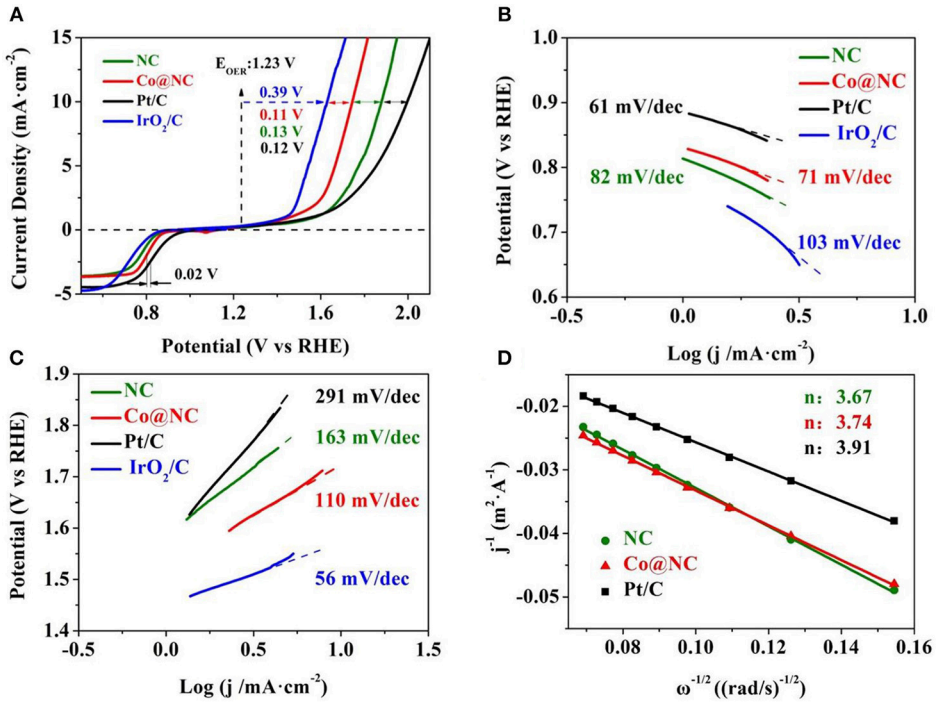

FIGURE 3 | (A) ORR and OER polarezation curves of Co@NC, NC, and Pt/C (electrolyte: O_2-saturated 0.1 M KOH, scan rate: 10 mV·s^{-1}, rotational speed: 1,600 rpm). Tafel plots of Co@NC, NC, Pt/C and IrO_2/C for **(B)** ORR; **(C)** OER. **(D)** Koutecky-Levich (K-L) plots of NC, Co@NC, and Pt/C at 0.5 V.

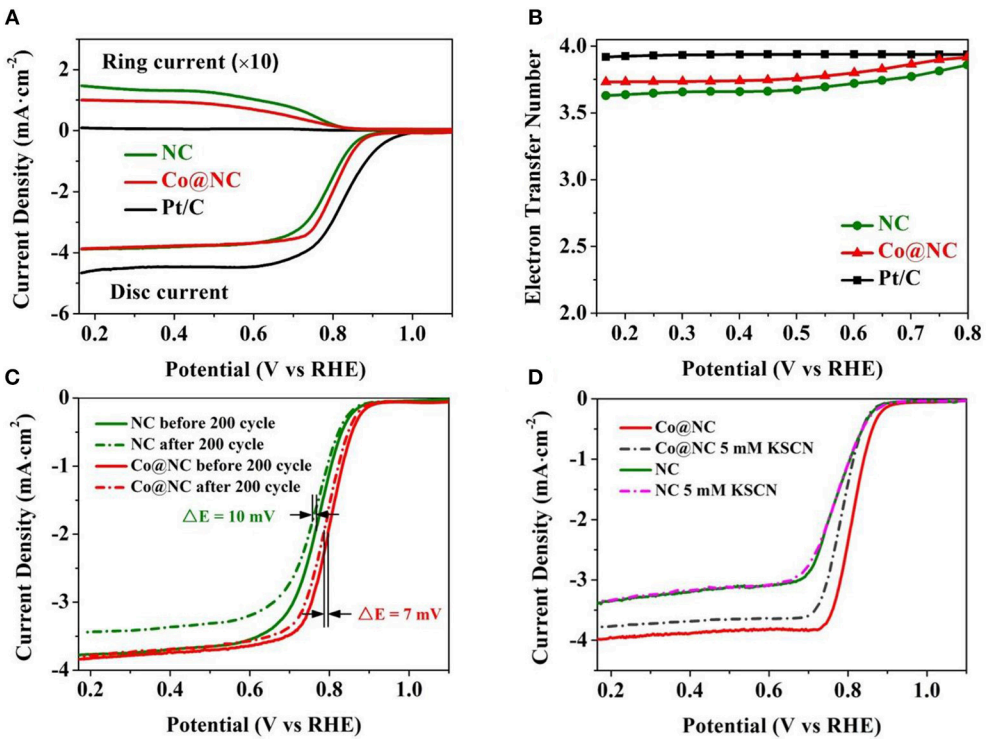

FIGURE 4 | (A) RRDE disk and ring currents recorded. **(B)** Electron transfer number of the Co@NC, NC and Pt/C (electrolyte: O_2-saturated 0.1 M KOH, scan rate: 10 mV·s^{-1}, rotational speed: 1,600 rpm). ORR polarization plots of **(C)** Co@NC and NC before and after continuously 200 cycles (electrolyte: O_2-saturated 0.1 M KOH). **(D)** Effect of KSCN interaction on the catalytic activity of Co@NC and NC.

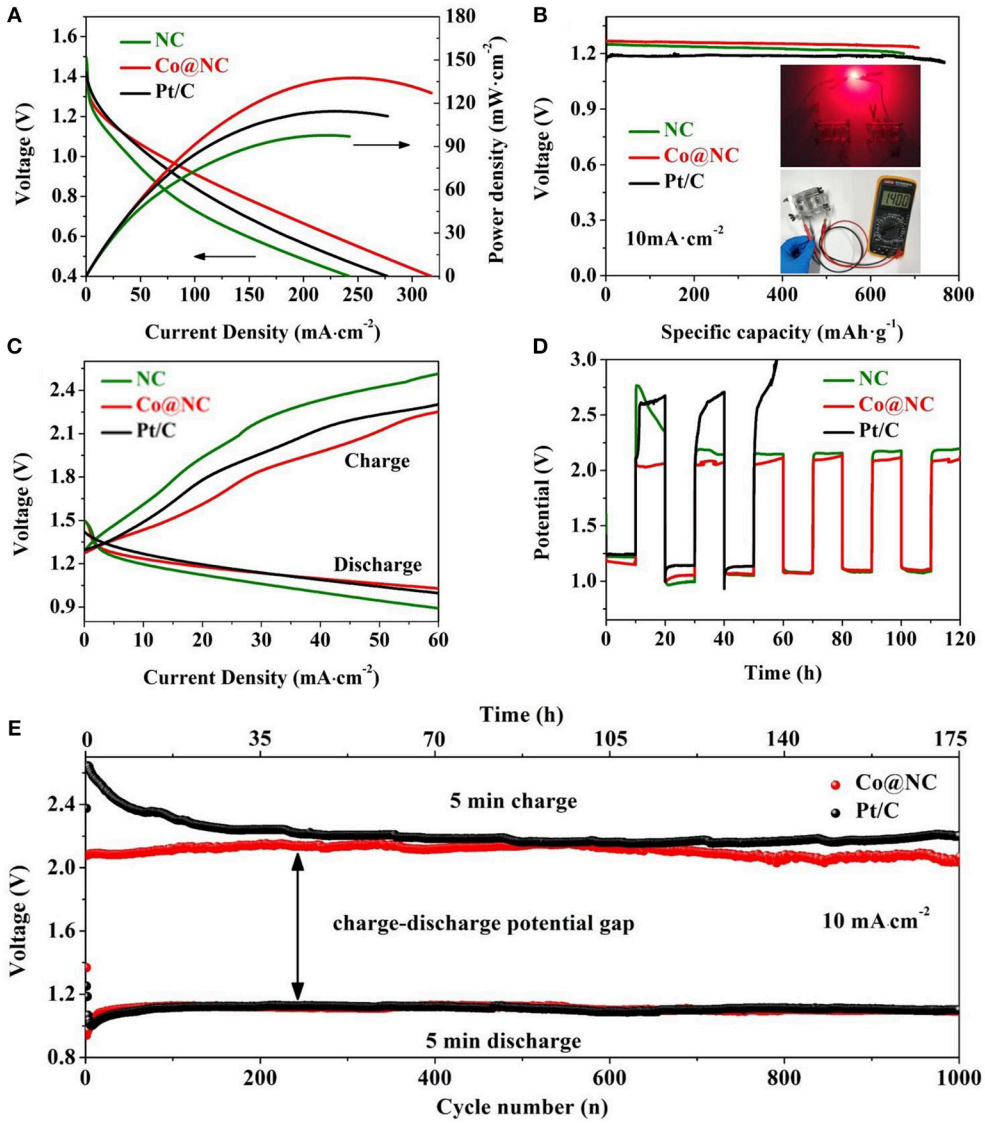

FIGURE 5 | (A) Discharge polarization curves and their corresponding power density curves. **(B)** Typical discharge curves of Co@NC, NC, and Pt/C based Zn-air batteries under continuous discharge until complete consumption of Zn. The illustrations are photograph of the assembled battery with an open-circuit voltage of 1.4 V and red LED powered in series by two rechargeable Zn-air batteries. **(C)** Charge/discharge polarization curves of the Co@NC, NC, and Pt/C catalyst, respectively. **(D)** Galvanostatic charge/discharge test of Co@NC, NC, and Pt/C based Zn-air battery (current density: 10 mA·cm^{-2}, cycle period: 20 h). **(E)** Charge/discharge cycling curves of Co@NC-based battery (current density: 10 mA·cm^{-2}, cycle period: 10 min).

Rechargeable Zn-Air Batteries

Superior bifunctional catalysts can accelerate the process of wide application of Zn-air batteries, and thus Co@NC was synthesized to build a typical Zn-air battery. In which, Co@NC electrocatalyst was loaded on conductive carbon paper (0.5 mg·cm^{-2}), Zn plate and 6 M KOH containing 0.2 M zinc acetate were used as the cathode, anode and electrolyte, respectively. **Figure 5A** presents polarization and power density curves of Co@NC, NC, and Pt/C electrocatalyst, Co@NC electrocatalyst exhibited a higher peak power density (137 mW·cm^{-2}) and a larger current density (246 mA·cm^{-2}) at 0.56 V, both of these are apparently higher than NC and Pt/C. Moreover, the Zn-air battery based on Co@NC electrocatalyst exhibits a large specific capacity of 708.3 mAh·g$_{Zn}^{-1}$ with a discharge platform of 1.27 V at 10 mA·cm^{-2} (**Figure 5B**), which is comparable to the specific capacity of Pt/C (767.1 mAh·g$_{Zn}^{-1}$), but is much larger than the specific capacity of NC (674.9 mAh·g$_{Zn}^{-1}$). By calculation we can also find that the energy density of Co@NC (868.9 mWh·g$_{Zn}^{-1}$) is slightly smaller than Pt/C (892.6 mWh·g$_{Zn}^{-1}$) but higher than NC (829.7 mWh·g$_{Zn}^{-1}$). Two Zn-air batteries were connected in series (**Figure 5B**), which can provide the required working voltage of the light-emitting diode (LED) and illuminate the rad LED in practical application. The results show that the air cathode of Co@NC can significantly improve the performance of the Zn-air battery than the others,

which is attributed to the superior ORR performance of Co@NC catalyst in alkaline medium (Fang et al., 2016b). Furthermore, in the charging process (OER process), Co@NC exhibited higher current density than Pt/C catalyst (**Figure 5C**), corresponding to the OER test result in **Figure 3A**.

Durability is an important indicator for future commercial applications of Zn-air batteries. Therefore, galvabostatic charge and discharge battery cycle were test at 10 $mA{\cdot}cm^{-2}$ in a 20 h cycle period in **Figure 5D**. The Zn-air battery with Co@NC electrocatalyst exhibit superior cycling stability. After 6 discharge/charging cycles, the total time exceeds 120 h, and the discharge/charging overpotential slightly changes. Comparatively speaking, the Zn-air battery based on Pt/C requires higher discharge/charge overpotential and <2 discharge/charge cycles (40 h). Besides that, the stability of Zn-air batteries with Co@NC, NC, and Pt/C catalysts were also evaluated at 10 $mA{\cdot}cm^{-2}$ with a 10 min cycle period (**Figure 5E** and **Figure S13**). It is worth noting that the charge/discharge overpotential (0.93 V) of Co@NC based Zn-air battery decreased slightly after 1,000 cycles. Which is smaller than the Zn-air battery with Pt/C (1.57 V) and NC(1.1 V). Although the Pt/C catalyst shows higher ORR kinetics, the degradation of the catalyst in charging process leads to a decline in continuous cycle activity. Above all, the as-prepared Co@NC electrocatalyst can be considered as a potential and more environmentally friendly catalyst that can be used as a substitute for noble metal catalysts for rechargeable metal-air batteries.

CONCLUSION

In summary, we developed a facile method for fabrication of nitrogen-doped carbon nanotube encapsulated with cobalt nanoparticles. In this process, DCDA and P123 were rational designed as the precursors and reducing agent to construct carbon nanotube and form cobalt nanoparitcles. The degree of graphitization of nitrogen-doped carbon strengthened in the presence of cobalt nanoparticles. The as obtained Co@NC electrocatalyst showed an excellent ORR and OER bifunctional electrocatalytic performance. In addition, the typical two-electrode Zn-air battery based on Co@NC electrocatalyst exhibited higher peak power density, large specific capacity and durability. The results of this paper provide a new strategy for the efficient production of nitrogen-doped carbon nanotube encapsulated cobalt. This method can be used in other energy storage devices, for instance, supercapacitors and fuel cells.

AUTHOR CONTRIBUTIONS

LH conceived the study designed the experiments. YL performed the experiments work, analyzed the data, and wrote the manuscript with the help from LH and YZ. HW performed the FESEM testing. PD, CZ, and ML analyzed the TEM data. All authors approved the manuscript for publication.

FUNDING

This work was supported by the National Natural Science Foundation of China (51802134, 51764029, and 51864024).

SUPPLEMENTARY MATERIAL

The Supplementary Material for this article can be found online at: https://www.frontiersin.org/articles/10.3389/fmats.2019.00085/full#supplementary-material

REFERENCES

Ai, L., Su, J., Wang, M., and Jiang, J. (2018). Bamboo-structured nitrogen-doped carbon nanotube co-encapsulating cobalt and molybdenum carbide nanoparticles: an efficient bifunctional electrocatalyst for overall water splitting. *ACS Sust. Chem. Eng.* 6, 9912–9920. doi: 10.1021/acssuschemeng.8b01120

Amiinu, I. S., Liu, X., Pu, Z., WenqiangLi, Li, Q., Jie, Z., Tang, H., et al. (2018). From 3D ZIF nanocrystals to Co-Nx/C nanorod array electrocatalysts for ORR, OER and Zn-air batteries. *Adv. Funct. Mater.* 28:1704638. doi: 10.1002/adfm.201704638

Cao, X., Zheng, X., Tian, J., Jin, C., Ke, K., and Yang, R. (2016). Cobalt sulfide embedded in porous nitrogen-doped carbon as a bifunctional electrocatalyst for oxygen reduction and evolution reactions. *Electrochim. Acta* 191, 776–783. doi: 10.1016/j.electacta.2016.01.137

Chen, J., Zhou, H., Huang, Y., Yu, H., Huang, F., Zheng, F., et al. (2016). A 3D Co-CN framework as a high performance electrocatalyst for the hydrogen evolution reaction. *RSC Adv.* 6, 42014–42018. doi: 10.1039/C6RA05632F

Dai, X., Li, Z., Ma, Y., Liu, M., Du, K., Su, H., et al. (2016). Metallic cobalt encapsulated in bamboo-like and nitrogen-rich carbonitride nanotubes for hydrogen evolution reaction. *ACS Appl. Mater. Interfaces* 8, 6439–6448. doi: 10.1021/acsami.5b11717

Deng, C., Zhong, H., Li, X., Yao, L., and Zhang, H. (2015). A highly efficient electrocatalyst for oxygen reduction reaction: phosphorus and nitrogen co-doped hierarchically ordered porous carbon derived from an iron-functionalized polymer. *Nanoscale* 8, 1580–1587. doi: 10.1039/C5NR06749A

Deng, D., Yu, L., Chen, X., Wang, G., Jin, L., Pan, X., et al. (2013). Iron Encapsulated within pod-like carbon nanotubes for oxygen reduction reaction. *Angew. Chem. Int. Edit.* 125, 389–393. doi: 10.1002/ange.201204958

Deng, H., Qian, L., Liu, J., and Feng, W. (2017). Active sites for oxygen reduction reaction on nitrogen-doped carbon nanotubes derived from polyaniline. *Carbon N. Y.* 112, 219–229. doi: 10.1016/j.carbon.2016.11.014

Dilpazir, S., He, H., Li, Z., Meng, W., Lu, P., Liu, R., et al. (2018). Cobalt single atoms immobilized N-doped carbon nanotubes for enhanced bifunctional catalysis toward oxygen reduction and oxygen evolution reactions. *ACS Appl. Energy Mater.* 1, 3283–3291. doi: 10.1021/acsaem.8b00490

Dong, S. H., He, D., Jing, W., Yue, L., Yin, P., Xun, H., et al. (2016). Ultrathin icosahedral Pt-enriched nanocage with excellent oxygen reduction reaction activity. *J. Am. Chem. Soc.* 138, 1494–1497. doi: 10.1021/jacs.5b12530

Fang, Y., Li, X., Li, F., Lin, X., Tian, M., Long, X., et al. (2016a). Self-assembly of cobalt-centered metal organic framework and multiwalled carbon nanotubes hybrids as a highly active and corrosion-resistant bifunctional oxygen catalyst. *J. Power Sources* 326, 50–59. doi: 10.1016/j.jpowsour.2016.06.11

Fang, Y., Wang, H., Hao, Y., and Feng, P. (2016b). From chicken feather to nitrogen and sulfur co-doped large surface bio-carbon flocs: an efficient electrocatalyst for oxygen reduction reaction. *Electrochim. Acta* 213, 273–282. doi: 10.1016/j.electacta.2016.07.121

Feng, Z., Wei, M., Jing, S., Chao, J., Yong, L., Bie, S., et al. (2018). Cobalt phosphide microsphere as an efficient bifunctional oxygen catalyst for Li-air batteries. *J Alloy. Compd.* 750, 655–658. doi: 10.1016/j.jallcom.2018.04.070

Guo, J., Niu, Q., Yuan, Y., Maitlo, I., Nie, J., and Ma, G. (2017). Electrospun core-shell nanofibers derived Fe-S/N depoed carbon material for oxygen reduction reaction. *Appl. Surf. Sci.* 416, 118–123. doi: 10.1016/j.apsusc.2017.04.135

Guo, S., Yuan, P., Zhang, J., Jin, P., Sun, H., Lei, K., et al. (2017). Atomic-scaled cobalt encapsulated in P, N-doped carbon sheaths over carbon nanotubes for enhanced oxygen reduction electrocatalysis under acidic and alkaline media. *Chem. Commun.* 53, 9862–9865. doi: 10.1039/C7CC05476A

Guo, Y., Yuan, P., Zhang, J., Hu, Y., Amiinu, I. S., Wang, X., et al. (2018b). Carbon nanosheets containing discrete Co-Nx-By-C active sites for efficient oxygen electrocatalysis and rechargeable Zn-air batteries. *ACS Nano* 12, 1894–1901. doi: 10.1021/acsnano.7b08721

Guo, Y., Yuan, P., Zhang, J., Xia, H., Cheng, F., Zhou, M., et al. (2018a). Co_2P-CoN double active centers confined in N-doped carbon nanotube: heterostructural engineering for trifunctional catalysis toward HER, ORR, OER, and Zn-air batteries driven water splitting. *Adv. Funct. Mater.* 28:1805641. doi: 10.1002/adfm.201805641

Hao, Y., Lu, Z., Zhang, G., Chang, Z., Luo, L., and Sun, X. (2017). Cobalt-embedded nitrogen doped carbon nanotubes as high performance bifunctional oxygen catalysts. *Energy Technol.* 5, 1265–1271. doi: 10.1002/ente.201600559

He, Q., Suraweera, N. S., Joy, D. C., and Keffer, D. J. (2013). Structure of the ionomer film in catalyst layers of proton exchange membrane fuel cells. *J. Phys. Chem. C* 117, 25305–25316. doi: 10.1021/jp408653f

Jie, Y., Zhong, Y., Wei, Z., and Shao, Z. (2017). Facile synthesis of nitrogen-doped carbon nanotubes encapsulating nickel cobalt alloys 3D networks for oxygen evolution reaction in an alkaline solution. *J. Power Sources* 338, 26–33. doi: 10.1016/j.jpowsour.2016.11.023

Karim, N. A., Kamarudin, S. K., and Loh, K. S. (2017). Performance of a novel non-platinum cathode catalyst for direct methanol fuel cells. *Energy Convers. Manag.* 145, 293–307. doi: 10.1016/j.enconman.2017.05.003

Kashyap, V., and Kurungot, S. (2018). Zirconium-substituted cobalt ferrite nanoparticle supported N-doped reduced graphene oxide as an efficient bifunctional electrocatalyst for rechargeable Zn-air battery. *ACS Catal.* 8, 3715–3726. doi: 10.1021/acscatal.7b03823

Li, J. S., Du, B., Lu, Z. H., Meng, Q. T., Sha, J. Q., Li, J. S., et al. (2017). *In situ*-generated Co@nitrogen-doped carbon nanotubes derived from MOFs for efficient hydrogen evolution in both alkaline and acidic conditions. *N. J. Chem.* 41, 10966–10971. doi: 10.1039/C7NJ02334K

Liang, Q., Jin, H., Wang, Z., Xiong, Y., Yuan, S., Zeng, X., et al. (2019). Metal-organic frameworks derived reverse-encapsulation Co-NC@Mo_2C complex for efficient overall water splitting. *Nano Energy* 57, 746–752. doi: 10.1016/j.nanoen.2018.12.060

Liu, Y., Lv, Y., and Cao, D. (2018). Co, N-codoped nanotube/graphene 1D/2D heterostructure for efficient oxygen reduction and hydrogen evolution reactions. *J. Mater. Chem. A* 6, 3926–3932. doi: 10.1039/C7TA11140A

Meng, F., Zhong, H., Bao, D., Yan, J., and Zhang, X. (2016). *In situ* coupling of strung Co_4N and intertwined N-C fibers toward free-standing bifunctional cathode for robust, efficient, and flexible Zn-air batteries. *J. Am. Chem. Soc.* 138, 10226–10231. doi: 10.1021/jacs.6b05046

Mo, Q., Chen, N., Deng, M., Yang, L., and Gao, Q. (2017). Metallic Cobalt@Nitrogen-doped carbon nanocomposites: carbon-shell regulation toward efficient Bi-functional electrocatalysis. *ACS Appl. Mater. Interfaces* 9, 37721–37730. doi: 10.1021/acsami.7b10853

Park, M. G., Lee, D. U., Seo, M. H., Cano, Z. P., and Chen, Z. (2016). 3D Ordered mesoporous bifunctional oxygen catalyst for electrically rechargeable zinc-air batteries. *Small* 12, 2707–2714. doi: 10.1002/smll.201600051

Qiao, X., Jin, J., Fan, H., Li, Y., and Liao, S. (2017). *In situ* growth of cobalt sulfide hollow nanospheres embedded in nitrogen and sulfur co-doped graphene nanoholes as a highly active electrocatalyst for oxygen reduction and evolution. *J. Mater. Chem. A* 5, 12354–12360. doi: 10.1039/C7TA00993C

Qiao, X., Liao, S., Zheng, R., Deng, Y., Song, H., and Du, L. (2016). Cobalt and nitrogen codoped graphene with inserted carbon nanospheres as an efficient bifunctional electrocatalyst for oxygen reduction and evolution. *ACS Sust. Chem. Eng.* 4, 4131–4136. doi: 10.1021/acssuschemeng.6b00451

Qu, K., Zheng, Y., Dai, S., and Qiao, S. Z. (2016). Graphene oxide-polydopamine derived N, S-codoped carbon nanosheets as superior bifunctional electrocatalysts for oxygen reduction and evolution. *Nano Energy* 19, 373–381. doi: 10.1016/j.nanoen.2015.11.027

Qu, K., Zheng, Y., Zhang, X., Davey, K., Dai, S., and Qiao, S. Z. (2017). Promotion of electrocatalytic hydrogen evolution reaction on nitrogen-doped carbon nanosheets with secondary heteroatoms. *ACS. Nano* 11, 7293–7300. doi: 10.1021/acsnano.7b03290

Sheng, J., Wang, L., Deng, L., Zhang, M., He, H., Zeng, K., et al. (2017). A MOF-templated fabrication of hollow Co_4N@N-doped carbon porous nanocages with superior catalytic activity. *ACS Appl. Mater. Interfaces* 10, 7191–7200. doi: 10.1021/acsami.8b00573

Si, C., Zhang, Y., Zhang, C., Gao, H., Ma, W., Lv, L., et al. (2017). Mesoporous nanostructured spinel-type MFe_2O_4 (M = Co, Mn, Ni) oxides as efficient bi-functional electrocatalysts towards oxygen reduction and oxygen evolution. *Electrochim. Acta* 245, 829–838. doi: 10.1016/j.electacta.2017.06.029

Song, A., Wang, Y., Wu, Y., Gang, S., Yin, X., Gao, L., et al. (2017). Facile synthesis of cobalt nanoparticles entirely encapsulated in slim nitrogen-doped carbon nanotubes as oxygen reduction catalyst. *ACS Sust. Chem. Eng.* 5, 3973–3981. doi: 10.1021/acssuschemeng.6b03173

Tao, A., Ge, X., Hor, T. S. A., Goh, F. W. T., Geng, D., Du, G., et al. (2015). Co_3O_4 nanoparticles grown on N-doped Vulcan carbon as a scalable bifunctional electrocatalyst for rechargeable zinc-air batteries. *RSC Adv.* 5, 75773–75780. doi: 10.1039/C5RA11047E

Tian, X., Luo, J., Nan, H., Zou, H., Chen, R., Shu, T., et al. (2016). Transition metal nitride coated with atomic layers of Pt as a low-cost, highly stable electrocatalyst for the oxygen reduction reaction. *J. Am. Chem. Soc.* 138, 1575–1583. doi: 10.1021/jacs.5b11364

Wang, R., Dong, X. Y., Du, J., Zhao, J. Y., and Zang, S. Q. (2018). MOF-derived bifunctional Cu_3P nanoparticles coated by a N, P-codoped carbon shell for hydrogen evolution and oxygen reduction. *Adv. Mater.* 30:1703711. doi: 10.1002/adma.201703711

Wang, Z., Xiao, S., An, Y., Long, X., Zheng, X., Lu, X., et al. (2016). $Co(II)_{1--x}Co(0)_{x/3}Mn(III)_{2x/3}S$ nanoparticles supported on B/N-codoped mesoporous nanocarbon as a bifunctional electrocatalyst of oxygen reduction/evolution for high-performance zinc-air batteries. *ACS Appl. Mater. Interfaces* 8, 13348–13359. doi: 10.1021/acsami.5b12803

Wei, C., Wang, H., Eid, K., Kim, J., Kim, J. H., Alothman, Z. A., et al. (2017). A three-dimensionally structured electrocatalyst: cobal-embedded nitrogen-doped carbon nanotubes/nitrogen-doped reduced graphene oxide hybrid for efficient oxygen reduction. *Chem-Eur. J.* 23, 637–643. doi: 10.1002/chem.201604113

Wen, L., Deng, Y. P., Li, G., Cano, Z. P., Wang, X., Dan, L., et al. (2018). Two-dimensional phosphorus-doped carbon nanosheets with tunable porosity for oxygen reactions in zinc-air batteries. *ACS Catal.* 8, 2464–2472. doi: 10.1021/acscatal.7b02739

Yang, X., Zheng, Y., Yang, J., Shi, W., Zhong, J. H., Zhang, C., et al. (2016). Modeling Fe/N/C catalysts in monolayer graphene. *Acs Catal.* 7, 139–145. doi: 10.1021/acscatal.6b0270

Yang, Z. K., Lin, L., Liu, Y.-N., Zhou, X., Yuan, C.-Z., and Xu, A.-W. (2016). Supramolecular polymers-derived nonmetal N, S-codoped carbon nanosheets for efficient oxygen reduction reaction. *RSC Adv.* 6, 52937–52944. doi: 10.1039/C6RA05523K

Zehtab, Y. A., Fei, H., Ye, R., Wang, G., Tour, J. M., and Sundararaj, U. (2015). Boron/nitrogen co-doped helically unzipped multiwalled carbon nanotubes as efficient electrocatalyst for oxygen reduction. *ACS Appl. Mater. Interfaces* 7, 7786–7794. doi: 10.1021/acsami.5b01067

Zhang, J., Zhao, Z., Xia, Z., and Dai, L. (2015). A metal-free bifunctional electrocatalyst for oxygen reduction and oxygen evolution reactions. *Nat. Nanotechnol.* 10, 444–452. doi: 10.1038/NNANO.2015.48

Zhao, J., and Chen, Z. (2015). Carbon-doped boron nitride nanosheet: an efficient metal-free electrocatalyst for the oxygen reduction reaction. *J. Phys. Chem. C* 119, 26348–26354. doi: 10.1021/acs.jpcc.5b09037

Zhe, W., Peng, S., Hu, Y., Li, L., Tao, Y., Yang, G., et al. (2017). Cobalt nanoparticles encapsulated in carbon nanotube-grafted nitrogen and sulfur co-doped multichannel carbon fibers as efficient bifunctional oxygen electrocatalysts. *J. Mater. Chem. A* 5, 4949–4961. doi: 10.1039/C6TA10291C

Zheng, Y., Jiao, Y., Zhu, Y., Cai, Q., Vasileff, A., Li, L. H., et al. (2017). Molecule-level g-C_3N_4 coordinated transition metals as a new class of

electrocatalysts for oxygen electrode reactions. *J. Am. Chem. Soc.* 139, 3336–3339. doi: 10.1021/jacs.6b13100

Zhou, L., Qu, X., Zheng, D., Tang, H., Liu, D., Qu, D., et al. (2017). Electrochemical hydrogen storage in facile synthesized Co@N-doped carbon nanoparticle composites. *ACS Appl. Mater. Interfaces* 9, 41332–41338. doi: 10.1021/acsami.7b14163

Zhou, T., Zhou, Y., Ma, R., Zhou, Z., Liu, G., Liu, Q., et al. (2017). Nitrogen-doped hollow mesoporous carbon spheres as a highly active and stable metal-free electrocatalyst for oxygen reduction. *Carbon* 114, 177–186. doi: 10.1016/j.carbon.2016.12.011

Zhou, W., Zhou, Y., Yang, L., Huang, J., Ke, Y., Zhou, K., et al. (2015). N-doped carbon-coated cobalt nanorod arrays supported on a titanium mesh as highly active electrocatalysts for hydrogen evolution reaction. *J. Mater. Chem. A* 3, 1915–1919. doi: 10.1039/C4TA06284A

Conflict of Interest Statement: The authors declare that the research was conducted in the absence of any commercial or financial relationships that could be construed as a potential conflict of interest.